Organic & Biomolecular Chemistry

PAPER

View Article Online
View Journal | View Issue

Cite this: *Org. Biomol. Chem.*, 2019, **17**, 2432

Salts accelerate the switching kinetics of a cyclobis(paraquat-*p*-phenylene) [2]rotaxane†

Sissel S. Andersen,[a] Afaf W. Saad,[a] Rikke Kristensen,[a] Teis S. Pedersen,[a] Luke J. O'Driscoll,[a] Amar H. Flood[b] and Jan O. Jeppesen*[a]

Received 13th January 2019,
Accepted 5th February 2019

DOI: 10.1039/c9ob00085b

rsc.li/obc

The rate at which the macrocyclic cyclobis(paraquat-*p*-phenylene) ring of a bistable [2]rotaxane moves from a tetrathiafulvalene station to an oxyphenylene station upon oxidation of the tetrathiafulvalene station is found to be increased in the presence of added salts. Compared to the salt-free case, 0.1 M solutions of a series of tetraalkylammonium hexafluorophosphate salts ($R_4N{\cdot}PF_6$, R = H, Me, Et or *n*-Bu) and of tetrabutylammonium perchlorate (*n*-$Bu_4N{\cdot}ClO_4$) all afford an increased switching rate, which is largest in the case of *n*-$Bu_4N{\cdot}ClO_4$ with smaller anions. Variation in the size of the ammonium cation has no significant effect. These results indicate that the addition of excess ions can be used as an accelerator to speed up shuttling processes in rotaxanes and catenanes based on the mobile cyclobis(paraquat-*p*-phenylene) ring, and that the choice of anion offers a convenient means of controlling the extent of this effect.

Introduction

The synthesis of [2]rotaxanes[1–6] and [2]catenanes[7–12] with the goal of making molecular shuttles has been an area of considerable research interest for more than twenty years. These systems consist of either a linear dumbbell in rotaxanes or a macrocyclic ring in catenanes as the 'track' along which an encircling macrocycle can move. By synthetic design of the 'track' it is possible to realise molecular machines capable of following a defined direction of motion.[13–15] For instance, the macrocycle of a [2]rotaxane can shuttle between different stations incorporated into the dumbbell 'track'. Initiation of this shuttling process requires an external stimulus (*e.g.* light,[16–18] addition of ions[19–21] or electrons,[22,23] *etc.*) to change the relative affinity of the stations for the macrocycle, thereby providing a driving force for the macrocycle to move and afford a new stable translational isomer. In order to exploit this motion efficiently, it is important to control the kinetics of the system. This control has previously been achieved by utilising sterically bulky groups[9] to completely block the pathway between two stations. "Speed bumps" based on sterics[22,24–26] or redox-switchable electrostatic barriers[27,28] have been used to control the kinetics of motion, as have photoswitchable gates and dynamic foldameric linker regions.[28] In an alternative approach, modifying the size of the macrocyclic ring has been found to have a significant effect on the kinetics of switching in rotaxanes.[29,30] It was recently found that kinetics are also influenced by changes to the length of linkers between stations.[31,32] Yet, the parameters available to vary the kinetics are still being discovered.

Tetrathiafulvalene (TTF) and its derivatives are electron-rich species that can be readily and reversible oxidised. Early interest in TTF derivatives related to the electronic properties of their charge transfer (CT) salts. More recently, the properties of the TTF unit have been widely utilised in supramolecular chemistry[33] and have found applications in other fields such as molecular electronics.[34,35] One of the most elegant applications of TTF derivatives is as stations in electroactive [2]rotaxanes. Cyclobis(paraquat-*p*-phenylene) ($CBPQT^{4+}$) is often used as the encircling macrocyclic ring in [2]rotaxanes.[22,36,37] One significant advantage of $CBPQT^{4+}$ is that it is a strong electron acceptor,[38] and therefore interacts favourably with electron donating stations such as TTF derivatives.[39–41] The redox properties of TTFs can be exploited to induce switching, as they can be reversibly oxidised to their cation radical ($TTF^{\bullet+}$) and dication (TTF^{2+}) states.[33,39,42–44] This oxidation replaces the favourable CT interactions between $CBPQT^{4+}$ and neutral TTF with a coulombic repulsion between two positively charged species, and can therefore be used to generate motion. When used in molecular machines, $CBPQT^{4+}$ typically has four hexafluorophosphate (PF_6^-) counterions on account of the resultant high solubility in MeCN, a favoured solvent for switching studies. It was previously shown that changing the anions associated with $CBPQT^{4+}$ affects the binding affinity between

[a]*Department of Physics, Chemistry and Pharmacy, University of Southern Denmark, Campusvej 55, DK 5230 Odense M, Denmark. E-mail: joj@sdu.dk; Tel: +45 65 50 25 87*

[b]*Chemistry Department, Indiana University, 800 E Kirkwood Avenue, Bloomington, IN 47405, USA*

†Electronic supplementary information (ESI) available: UV-Vis-NIR and ^{1}H NMR spectra, kinetic data and differential pulse voltammogram of **1**·4PF_6. See DOI: 10.1039/c9ob00085b

$CBPQT^{4+}$ and a TTF or monopyrrolo-TTF guest;[45] replacing PF_6^- with larger anions enhanced the performance of $CBPQT^{4+}$ as a π-electron acceptor whereas smaller anions showed the opposite effect. Increasing the concentration of the anions by adding 0.1 M tetrabutylammonium hexafluorophosphate (n-$Bu_4N{\cdot}PF_6$) was found to decrease the binding affinity. This effect was attributed to a shift in the ion-pair equilibrium (*e.g.* $CBPQT^{4+} + 4PF_6^- \rightleftarrows CBPQT{\cdot}4PF_6$) to favour increased association of the PF_6^- anions with the tetracationic $CBPQT^{4+}$ macrocycle.[45] As a consequence, the net interactions between $CBPQT^{4+}$ and the TTF-based stations were weakened. These results, along with the observation that varying the anions associated with $CBPQT^{4+}$ in a bistable [2]rotaxane changes the ratio between its two translational isomers,[46] led us to hypothesise that the addition of anions of different sizes and concentrations would make it possible to adjust the kinetics of a suitably designed [2]rotaxane based on $CBPQT^{4+}$ and TTF.

If the presence of ions indeed makes a difference to the kinetics of [2]rotaxanes, it is important to consider this effect when comparing measurements between different techniques. For instance, cyclic voltammetry (CV) measurements generally require the presence of a supporting electrolyte (typically a 0.1 M salt solution)[47–49] whereas UV-Vis-NIR absorption or NMR spectroscopy studies are usually conducted in high-purity, additive-free solvent. Indeed, comparison of results from CV studies with those from other techniques is known to be far from straightforward.[50]

Many examples of [2]rotaxanes and [2]catenanes in which shuttling[19,20] or rotation[51] processes are induced by ion exchange are known. However, to the best of our knowledge, there are no examples in the literature in which ions are used to intentionally accelerate or decelerate the rate of the shuttling process of a macrocyclic ring between different stations. Such control of kinetics is important in order to develop systems in which movement of the ring component can be performed in a controlled manner.

We investigate the effect that the presence of additional ions has on the behaviour of the [2]rotaxane $1{\cdot}4PF_6$ (Fig. 1). Specifically, we examine how the ionic environment changes the kinetics of movement of the $CBPQT^{4+}$ macrocycle from the central TTF station (green) to the outer oxyphenylene (OP) stations (red) upon oxidation of the TTF unit. By using UV-Vis-NIR absorption spectroscopy to measure the kinetics,[26] it is possible to compare systems both with and without added salts. Kinetics were determined in the presence of no additional ions, with a series of $R_4N{\cdot}PF_6$ salts (R = H, Me, Et and *n*-Bu) and using n-$Bu_4N{\cdot}ClO_4$. The data shows that the additional salts accelerate the switching rate and that the choice of anion can modulate this effect. Addition of an appropriate salt can enhance the switching rate of the [2]rotaxane $1{\cdot}4PF_6$ following oxidation by a factor of more than three.

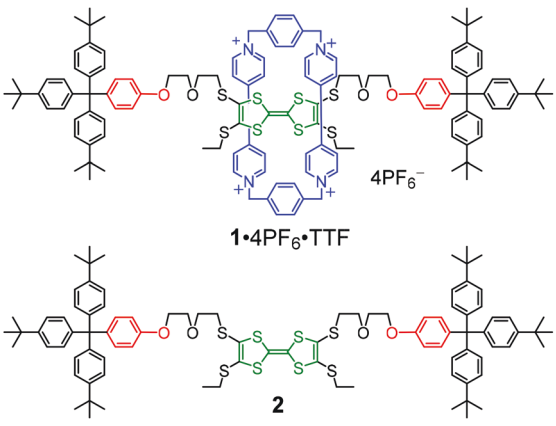

Fig. 1 Structures of the [2]rotaxane $1{\cdot}4PF_6{\cdot}$TTF and its precursor dumbbell **2**. Both compounds exist as a mixture of *E* and *Z* isomers.

Results and discussion

Design and synthesis

The [2]rotaxane $1{\cdot}4PF_6$ was synthesised according to the reported procedure.[32] It is symmetrical and contains two types of stations around which the $CBPQT^{4+}$ macrocycle can reside: a TTF station (green, Fig. 1) located at the center of the dumbbell and two equivalent weakly-binding OP stations[32] (red, Fig. 1), which are part of the bulky stopper groups at the ends of the dumbbell. The OP stations are suitable binding sites for $CBPQT^{4+}$, but much weaker than the neutral TTF station.‡ However, the OP stations are much more preferable binding sites than an oxidised TTF unit. The [2]rotaxane $1{\cdot}4PF_6$ was chosen for this study as the ground-state co-conformation exists almost exclusively as the isomer in which $CBPQT^{4+}$ binds to the TTF station (*i.e.* $1{\cdot}4PF_6{\cdot}$TTF as illustrated in Fig. 1), which allows for extremely efficient studies of switching thermodynamics. Additionally, the thioethyl (SEt) barrier is of an appropriate size[26] to monitor the movement of $CBPQT^{4+}$ away from the TTF station upon oxidation using UV-Vis-NIR absorption spectroscopy.

^{1}H NMR spectroscopy

A ^{1}H NMR spectrum (400 MHz, 298 K) recorded in CD_3CN of the [2]rotaxane $1{\cdot}4PF_6$ reveals (Fig. S9†) that it almost exclusively exists (>95%) as the translational isomer $1{\cdot}4PF_6{\cdot}$TTF in which $CBPQT^{4+}$ encircles the TTF station. This observation is supported by the fact that the binding between $CBPQT{\cdot}4PF_6$ and the OP unit is very low (ΔG° = −1.7 kcal mol^{-1})[32] in CD_3CN at 298 K as compared to the binding between $CBPQT{\cdot}4PF_6$ and the TTF unit (ΔG° = −4.4 kcal mol^{-1})[32] in MeCN at 298 K. Assuming that the relative populations between $1{\cdot}4PF_6{\cdot}$OP and $1{\cdot}4PF_6{\cdot}$TTF are related to the free energy difference ($\Delta\Delta G^\circ$) for the binding between $CBPQT^{4+}$ and the TTF thread and a pseudodumbbell containing the OP

‡ ΔG° values of −4.4 kcal mol^{-1} (MeCN, 298 K) and −1.7 kcal mol^{-1} (CD_3CN, 298 K) for the binding between $CBPQT^{4+}$ and a TTF thread and between $CBPQT^{4+}$ and a pseudodumbbell containing the OP station, respectively, have been reported.[32]

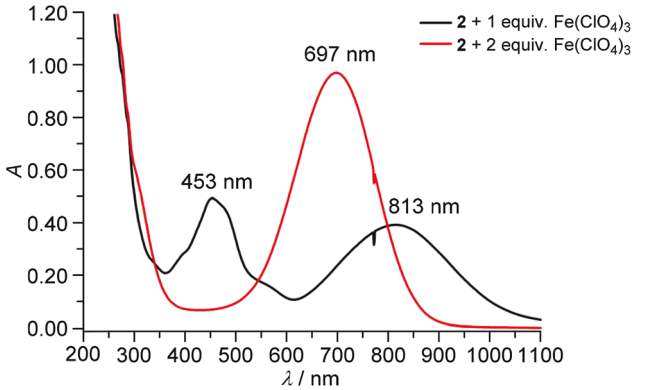

Fig. 2 UV-Vis-NIR absorption spectra of **2** (0.1 mM) in MeCN at 298 K recorded upon addition of 1.0 equiv. of $Fe(ClO_4)_3$ (black) and 2.0 equiv. of $Fe(ClO_4)_3$ (red).

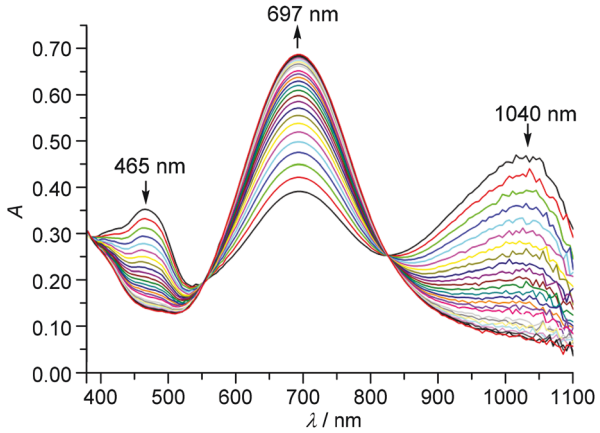

Fig. 3 Time lapse absorption spectra recorded of **1**·4PF_6 (0.1 mM) in MeCN at 298 K after addition of 1.0 equiv. of $Fe(ClO_4)_3$. The first spectrum (black line) was recorded *ca.* 7 min after addition of $Fe(ClO_4)_3$ and subsequent spectra at 45 s intervals.

station, respectively, a calculated isomer distribution of 1% **1**·4PF_6·OP and 99% **1**·4PF_6·TTF can be obtained.

UV-Vis-NIR oxidation studies

In order to follow the behaviour of $\mathbf{1}^{4+}$ using UV-Vis-NIR absorption spectroscopy, it was important to first have a good understanding of the absorption bands associated with the oxidised states of the precursor dumbbell **2** (Fig. 1). The UV-Vis-NIR absorption spectra (Fig. 2, MeCN, 298 K) of **2** recorded after the addition of either 1.0 (black line) or 2.0 (red line) equiv. of $Fe(ClO_4)_3$ have well resolved absorption bands attributed to the oxidised species. The monocationic oxidised species $\mathbf{2}^{\bullet+}$ has absorption bands at 453 and 813 nm, while the dication $\mathbf{2}^{2+}$ has an absorption band at 697 nm.

Adding 1.0 equiv. of $Fe(ClO_4)_3$ to a solution of the [2]rotaxane $\mathbf{1}^{4+}$ gives the singly-oxidised monocationic form of the TTF, $\mathbf{1}^{5+/1\bullet}$ (Scheme 1) over a couple of minutes (Fig. S1†). This is evidenced by the appearance of absorption bands at 465 and 1040 nm (Fig. 3). These bands are redshifted by 12 and 227 nm, respectively, compared to the free dumbbell $\mathbf{2}^{\bullet+}$ (453 and 813 nm, Fig. 2), indicating that the mono-oxidised cation radical $TTF^{\bullet+}$ unit remains inside the cavity of $CBPQT^{4+}$ after the first oxidation. This observation indicates that at room temperature the SEt barriers must be too large to permit $CBPQT^{4+}$ to pass over them immediately after the formation of $TTF^{\bullet+}$, despite the coulombic repulsion between the positively charged $TTF^{\bullet+}$ unit and the $CBPQT^{4+}$ ring.

When the oxidised solution is monitored over a longer time (Fig. 3), the absorption bands assigned to $\mathbf{1}^{5+/1\bullet}$ (465 and 1040 nm) decrease in intensity while an additional absorption band at 697 nm simultaneously increases in intensity. The band at 697 nm has the same absorption maximum as that of

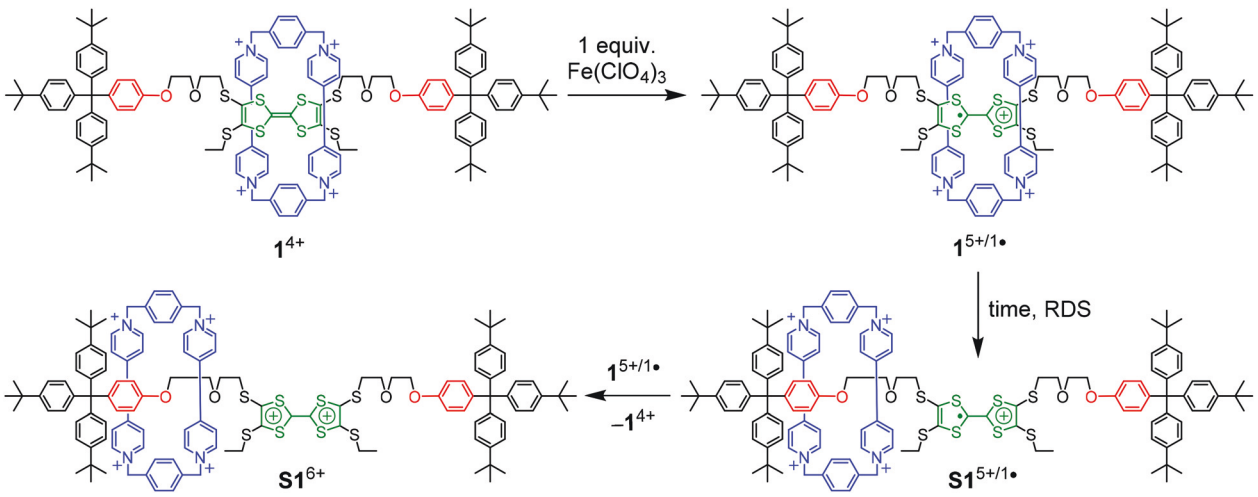

Scheme 1 The effect of adding 1.0 equiv. of $Fe(ClO_4)_3$ to the rotaxane $\mathbf{1}^{4+}$. Firstly, the mono-oxidised rotaxane $\mathbf{1}^{5+/1\bullet}$ is formed. Secondly, switching of $\mathbf{1}^{5+/1\bullet}$ generates the switched form of the [2]rotaxane $\mathbf{S1}^{5+/1\bullet}$, which disproportionates to generate the initial, ground state rotaxane $\mathbf{1}^{4+}$ and the doubly-oxidised switched compound $\mathbf{S1}^{6+}$. RDS = Rate determining step.

the doubly-oxidised dumbbell 2^{2+} (Fig. 2), indicating that it relates to a TTF unit in the dication state (*i.e.* TTF^{2+}) which is not encircled by $CBPQT^{4+}$. It follows that the switched, doubly-oxidised [2]rotaxane $\mathbf{S1}^{6+}$ (Scheme 1), where $CBPQT^{4+}$ encircles one of the OP stations in the stopper unit, must form over time. This requires both switching of the [2]rotaxane to its other translational isomer ($\mathbf{1}^{5+/1\bullet}$ to $\mathbf{S1}^{5+/1\bullet}$) and a disproportionation reaction ($\mathbf{1}^{5+/1\bullet}$ and $\mathbf{S1}^{5+/1\bullet}$ to $\mathbf{1}^{4+}$ and $\mathbf{S1}^{6+}$). Based on electrochemical studies (*vide infra*), the disproportionation occurs after $CBPQT^{4+}$ moves from the TTF station to an OP station, *i.e. via* the route illustrated in Scheme 1, with a driving force of *ca.* 160 mV. A similar disproportionation reaction has previously been reported with a much smaller driving force (<20 mV).[26]

Addition of 2.0 equiv. of $Fe(ClO_4)_3$ to $\mathbf{1}^{4+}$ was found to be insufficient to fully oxidise all $\mathbf{1}^{4+}$ to $\mathbf{1}^{6+}$ or $\mathbf{S1}^{6+}$. This observation can most likely be accounted for by the fact that when $\mathbf{1}^{5+/1\bullet}$ forms, $CBPQT^{4+}$ still surrounds the $TTF^{\bullet+}$ unit in $\mathbf{1}^{5+/1\bullet}$, which makes the second oxidation more difficult (as evidenced by the redox potentials in the electrochemical studies section below). However, an excess of $Fe(ClO_4)_3$ allowed for complete switching of $\mathbf{1}^{4+}$ to $\mathbf{1}^{6+}$. In this case, it appears that after $\mathbf{1}^{6+}$ forms, the electrostatic repulsion between TTF^{2+} and $CBPQT^{4+}$ is strong enough that the SEt barrier is overcome rapidly, as the system switches to $\mathbf{S1}^{6+}$ within the time needed to record a UV-Vis-NIR spectrum (Fig. S2†). It is therefore not possible to measure the switching from $\mathbf{1}^{6+}$ to $\mathbf{S1}^{6+}$ using UV-Vis-NIR absorption spectroscopy (at least not at temperatures close to room temperature).

Electrochemical studies

Cyclic voltammograms (CVs) of the [2]rotaxane $\mathbf{1}\cdot 4PF_6$ and its corresponding dumbbell **2** were recorded (Fig. 4) in MeCN (1 : 2 DCE/MeCN in the case of **2** because of its low solubility in neat MeCN) at 298 K. The obtained oxidation (E_{ox}), reduction (E_{red}) and half-wave ($E_{1/2}$) potentials are summarised in Table 1. Dumbbell **2** shows a pair of characteristic single-electron reversible redox processes at $E_{1/2}$ = +0.16 and +0.46 V *vs.* Fc/Fc^+, assigned to the first and second oxidations of the TTF unit, respectively. The [2]rotaxane $\mathbf{1}\cdot 4PF_6$ shows a four-wave pattern in the outward sweep of the CV, with oxidation peaks at E_{ox} = +0.19, +0.41, +0.57 and +0.94 V. The first two oxidation peaks are very similar (Table 1) to the oxidation peaks of the dumbbell **2** indicating that in this case $CBPQT^{4+}$ does not encircle the TTF unit. Consequently, these processes can be associated with the first and second oxidations of the TTF unit in $\mathbf{1}\cdot 4PF_6$·OP. The last two processes at E_{ox} = +0.57 and +0.94 V *vs.* Fc/Fc^+ can be assigned to the first and second oxidation of the TTF unit in $\mathbf{1}\cdot 4PF_6$·TTF since they are shifted anodically by +0.41 and +0.48 V, respectively, compared to the oxidation peaks of the dumbbell **2**.§

A differential pulse voltammogram (DPV) of the [2]rotaxane $\mathbf{1}\cdot 4PF_6$ recorded in MeCN at 298 K was used to determine the ratio of $\mathbf{1}\cdot 4PF_6$·OP and $\mathbf{1}\cdot 4PF_6$·TTF present in the [2]rotaxane $\mathbf{1}\cdot 4PF_6$. The DPV (Fig. S10†) revealed three peaks at +0.14, +0.52 and +0.90 V *vs.* Fc/Fc^+, integrating to 0.004, 0.224 and 0.050, respectively. Based on the results obtained from CV, the small DPV peak at +0.14 V can be assigned to first oxidation of the TTF unit in $\mathbf{1}\cdot 4PF_6$·OP, whereas the process observed at +0.52 V can be assigned to the coincidence of the second oxidation of the TTF unit in $\mathbf{1}\cdot 4PF_6$·OP and the first oxidation of the TTF unit in $\mathbf{1}\cdot 4PF_6$·TTF. Finally, the DPV peak at +0.90 V¶ can be assigned to the second oxidation of the TTF unit in $\mathbf{1}\cdot 4PF_6$·TTF. By using the DPV peak areas for the processes at +0.14 and +0.52 V, a calculated isomer distribution of 2% $\mathbf{1}\cdot 4PF_6$·OP and 98% $\mathbf{1}\cdot 4PF_6$·TTF can be obtained.‖ These results are fully consistent with the results obtained from NMR spectroscopy (*vide supra*).

The fact that the second oxidation peak of $\mathbf{1}\cdot 4PF_6$·TTF is 0.48 V more positive than the second oxidation peak of the dumbbell **2** clearly indicates that the $CBPQT^{4+}$ ring remains around the cation radical $TTF^{\bullet+}$ unit on the timescale of the CV experiment.[52] This observation is in full agreement with the results obtained from the UV-Vis-NIR absorption spectroscopy study (*vide supra*), which showed that the switching from $\mathbf{1}^{5+/1\bullet}$ to $\mathbf{S1}^{5+/1\bullet}$ did not take place immediately after oxidation but happened over a few minutes.

Finally, the CV data unambiguously show that the oxidation of $\mathbf{S1}^{5+/1\bullet}$ to $\mathbf{S1}^{6+}$ (+0.41 V) takes place at a potential that is *ca.* 160 mV lower than the first oxidation of $\mathbf{1}^{4+}$ (+0.57 V). Consequently, it is possible for $\mathbf{1}^{5+/1\bullet}$ to oxidise $\mathbf{S1}^{5+/1\bullet}$ to $\mathbf{S1}^{6+}$ which supports the proposed disproportionation reaction (*vide*

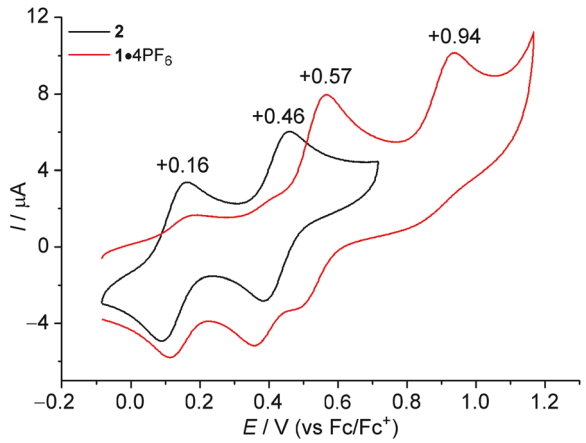

Fig. 4 Cyclic voltammograms of the dumbbell **2** (black) and [2]rotaxane $\mathbf{1}\cdot 4PF_6$ (red). The measurements were carried out at 298 K in nitrogen-purged solutions, either 0.4 mM in 1 : 2 DCE/MeCN (**2**) or 0.5 mM in MeCN ($\mathbf{1}\cdot 4PF_6$), with n-$Bu_4N\cdot PF_6$ as the electrolyte (0.1 M), a glassy carbon electrode as the working electrode and at a scan rate of 0.1 V s^{-1}.

§While the two redox processes associated with the [2]rotaxane $\mathbf{1}\cdot 4PF_6$·OP and the first redox process associated with the [2]rotaxane $\mathbf{1}\cdot 4PF_6$·TTF are all reversible, it should be noted that the second redox process associated with the [2]rotaxane $\mathbf{1}\cdot 4PF_6$·TTF appears to be irreversible.

¶It should be noted that the DPV peak area (0.050) for the process at +0.90 V is significantly lower than for the process at +0.52 V although it in theory should be 0.224–0.004 = 0.220. This observation can most likely be accounted for by the fact that the second oxidation process in $\mathbf{1}\cdot 4PF_6$·TTF is irreversible.

‖% ($\mathbf{1}\cdot 4PF_6$·OP) = (0.00404/0.22432) × 100% = 2% and % ($\mathbf{1}\cdot 4PF_6$·TTF) = ((0.22432–0.00404)/0.22432) × 100% = 98%.

Table 1 Electrochemical data for the dumbbell **2** and the [2]rotaxane **1**·4PF$_6$ obtained by cyclic voltammetry[a] (CV) at 298 K in MeCN (*vs.* Fc/Fc$^+$)

Compound	E^1_{ox} [b] [V]	E^2_{ox} [b] [V]	E^1_{red} [c] [V]	E^2_{red} [c] [V]	$E^1_{1/2}$ [d] [V]	$E^2_{1/2}$ [d] [V]
2	+0.16	+0.46	+0.10	+0.40	+0.13	+0.43
1·4PF$_6$·OP	+0.19	+0.41	+0.12	+0.36	+0.16	+0.39
1·4PF$_6$·TTF	+0.57	+0.94	+0.51	—	+0.54	—[e]

[a] CV measurements of **1**·4PF$_6$ (0.5 mM in nitrogen-purged MeCN) and **2** (0.4 mM in nitrogen-purged DCE : MeCN (1 : 2)) were conducted with 0.1 M *n*-Bu$_4$N·PF$_6$ as the electrolyte, a glassy carbon electrode as the working electrode, a Pt counter electrode and with a scan rate of 0.1 V s^{-1}; E_{ox}, E_{red} and $E_{1/2}$ values *vs.* Fc/Fc$^+$ and the estimated errors on the *E* values are ±0.01 V. [b] Anodic oxidation peak. [c] Cathodic reduction peak. [d] Half-wave potential, $E_{1/2} = (E_{ox} - E_{red})/2$. [e] Irreversible process.

supra) where **1**$^{5+/\bullet}$ and **S1**$^{5+/1\bullet}$ are converted into **1**$^{4+}$ and **S1**$^{6+}$, respectively.

UV-Vis-NIR kinetic studies

Having determined the switching mechanism of **1**$^{4+}$ upon oxidation and the characteristic UV-Vis-NIR absorption features, we set out to investigate the kinetics of the switching process and to probe the effect of added salts. Initial experiments were conducted in the absence of additional salts or in the presence of either 0.1 M *n*-Bu$_4$N·PF$_6$ or 0.1 M *n*-Bu$_4$N·ClO$_4$. *n*-Bu$_4$N·PF$_6$ is a very common supporting electrolyte in CV measurements,[48] so it is of interest to determine whether its presence affects switching kinetics. Furthermore, as the counterions in **1**·4PF$_6$ are the same as this salt, any possible effects resulting from ion exchange can be excluded. *n*-Bu$_4$N·ClO$_4$ is an alternative supporting electrolyte and allows for the effects of a change of anion to be probed, although in this case ion exchange is expected to occur on account of the large excess of added salt. Evidence of this ion exchange can be observed using ^{1}H NMR spectroscopy (Fig. S8†). It has previously been established that the addition of 0.1 M solutions of these salts reduces the binding affinity of a TTF derivative for CBPQT^{4+} relative to salt-free conditions.[45] By following the decrease of the absorption band from **1**$^{5+/1\bullet}$ at 1040 nm** after oxidation of **1**$^{4+}$ with 1.0 equiv. of Fe(ClO$_4$)$_3$, the rate at which CBPQT^{4+} moves over an SEt barrier to an OP station to form initially **S1**$^{5+/1\bullet}$ and subsequently **S1**$^{6+}$ can be determined.[32] The absorption at 1040 nm was recorded at intervals of 10 s (or less) in order to determine the rate constant with the highest possible precision (Fig. 5, 6 and Fig. S3, S4†). There is an initial lag period before all **1**$^{4+}$ is oxidised to **1**$^{5+/1\bullet}$ and the selected data points (Table 2) used to construct linear plots (Fig. 6) of ln *A* against time (*t*) were therefore those collected after the absorbance (*A*) had reached a maximum (Fig. 5).

The observed rate constant ($k_{observed}$) was calculated using first order kinetics at a range of temperatures (Table 2) in order to determine the enthalpic and entropic contributions to the kinetic barrier when CBPQT^{4+} moves away from a mono-oxidised TTF unit (TTF$^{\bullet+}$) over an SEt barrier to an OP unit to form **S1**$^{5+/1\bullet}$. The observed rate constants ($k_{observed}$) are four times larger than the true rate constants (*k*) of the switching process. This is because (i) CBPQT^{4+} can move across either of the two equivalent SEt barriers after oxidation of TTF (**1**$^{4+}$) to TTF$^{\bullet+}$ (**1**$^{5+/1\bullet}$) and (ii) only half of the oxidised molecule **1**$^{5+/1\bullet}$ forms the switched product **S1**$^{6+}$, with the remainder being reduced to **1**$^{4+}$ in the disproportionation reaction described above (Scheme 1). From the intrinsic rate constant *k*, it is pos-

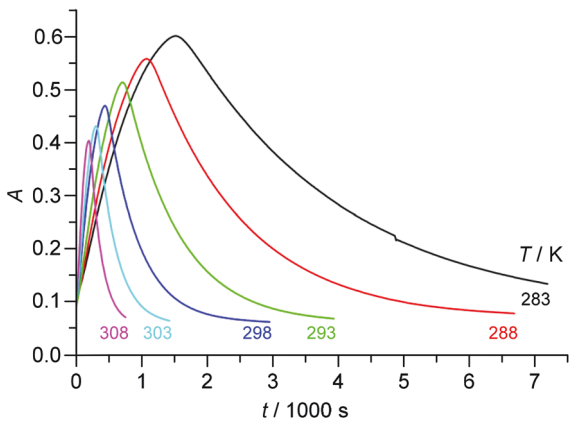

Fig. 5 Absorption measured at 1040 nm after addition of 1.0 equiv. Fe(ClO$_4$)$_3$ to a solution of **1**·4PF$_6$ (0.1 mM) in MeCN, as a function of time at six different temperatures.

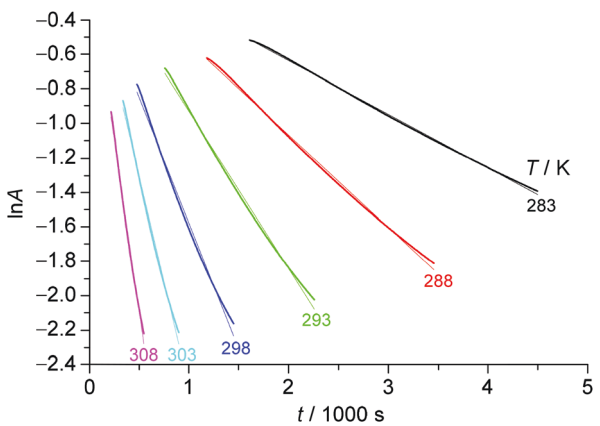

Fig. 6 Linear plots of ln *A* against *t* at six different temperatures after the addition of 1.0 equiv. of Fe(ClO$_4$)$_3$ to a solution of **1**·4PF$_6$ (0.1 mM) in MeCN obtained by using the absorption at 1040 nm as the probe. The data points have been fitted by best straight lines, giving correlation coefficients of 0.995–0.999, indicating that first order kinetics are in operation. The slope of each line gives the $k_{observed}$ value, according to the relationship $\ln A = -k_{observed}t$.

** No other bands interfere with this band.

Table 2 Rate constants (k) and derived $\Delta G^{\ddagger}$ values for the switching of CBPQT^{4+} from the TTF$^{\bullet+}$ unit in $\mathbf{1}^{5+/1\bullet}$ to the OP unit in $\mathbf{S1}^{5+/1\bullet}$ in MeCN at six different temperatures[a]

T [K]	Time selected [s]	Time between data points [s]	n	R^2	$k_{observed}$ [$\times 10^{-4}$ s^{-1}]	k [$\times 10^{-4}$ s^{-1}]	$\Delta G^{\ddagger}$ [kcal mol^{-1}]
283.0	1610–4500	10	290	0.999	3.11 ± 0.10	0.78 ± 0.02	21.88 ± 0.03
288.0	1180–3460	10	229	0.998	5.36 ± 0.18	1.34 ± 0.04	21.96 ± 0.03
288.0	1103–3683	10	259	0.997	5.21 ± 0.20	1.30 ± 0.05	21.98 ± 0.03
293.0	760–2260	10	151	0.997	9.12 ± 0.23	2.28 ± 0.06	22.05 ± 0.03
298.0	520–1400	10	89	0.997	14.8 ± 0.36	3.70 ± 0.09	22.14 ± 0.03
298.0	480–1450	10	98	0.995	14.6 ± 0.39	3.65 ± 0.10	22.15 ± 0.03
303.0	340–900	10	57	0.995	24.5 ± 0.68	6.13 ± 0.17	22.22 ± 0.03
308.0	220–550	10	34	0.996	39.9 ± 1.24	9.98 ± 0.31	22.30 ± 0.03

[a] The observed rate constants ($k_{observed}$) were obtained from UV-Vis-NIR absorption spectroscopy data using the absorption band at 1040 nm as a probe and $k = k_{observed}/4$. The $\Delta G^{\ddagger}$ values were calculated using the relationship $\Delta G^{\ddagger} = -RT\ln(kh/k_BT)$, where R is the gas constant, T is the absolute temperature, k is the rate constant, h is Planck's constant and k_B is the Boltzmann constant. The errors were calculated[53] using $\Delta T = 0.3$ K, $\Delta t = 0.1$ s and $\Delta A = 0.1\%$. n is the number of data points used to obtain $k_{observed}$.

sible to calculate the size of the kinetic barriers ($\Delta G^{\ddagger}$) at different temperatures; these values are shown in Table 2 and Tables S1 and S2† (for no additional salt, 0.1 M n-Bu$_4$N·PF$_6$ and 0.1 M n-Bu$_4$N·ClO$_4$, respectively). The enthalpic ($\Delta H^{\ddagger}$) and entropic ($\Delta S^{\ddagger}$) contributions to the kinetic barrier were calculated by plotting (Fig. 7) the barrier size ($\Delta G^{\ddagger}$) as a function of temperature (T). The resulting values are summarised in Table 3. It is evident that the addition of 0.1 M n-Bu$_4$N·PF$_6$ increases the rate constant (k) by 80% but the enthalpic and entropic contributions do not change significantly within experimental error. This indicates that the mechanism of switching is most likely the same, but that the excess PF_6^- anions have a stabilising effect on the transition state. Upon changing the salt from n-Bu$_4$N·PF$_6$ to n-Bu$_4$N·ClO$_4$, *i.e.* reducing the size of the anions, the rate constant (k) doubles, indicating that smaller anions have a more substantial stabilising

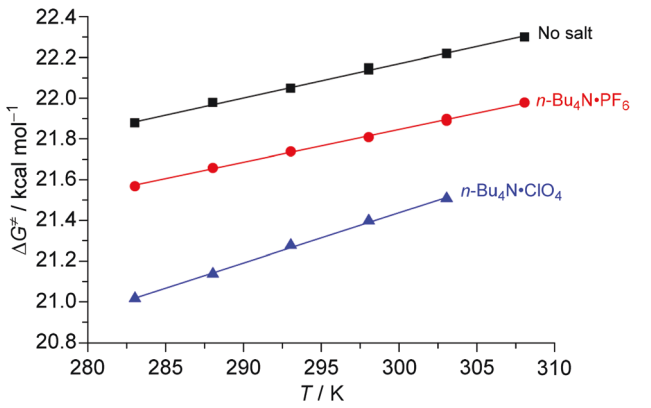

Fig. 7 The derived $\Delta G^{\ddagger}$ values as a function of temperature (T) for the switching of $\mathbf{1}^{5+/1\bullet}$ to $\mathbf{S1}^{5+/1\bullet}$ with and without added salts. Black, red and blue lines correspond to measurements made without salt, with 0.1 M n-Bu$_4$N·PF$_6$ and with 0.1 M n-Bu$_4$N·ClO$_4$, respectively. The slope and intercept of the linear regression analysis give the values $-\Delta S^{\ddagger}$ and $\Delta H^{\ddagger}$, respectively, from the equation $\Delta G^{\ddagger} = \Delta H^{\ddagger} - T \times \Delta S^{\ddagger}$. (The derived $\Delta G^{\ddagger}$ values can be found in Table 2 for no salt, Table S1† for n-Bu$_4$N·PF$_6$ and Table S2† for n-Bu$_4$N·ClO$_4$).

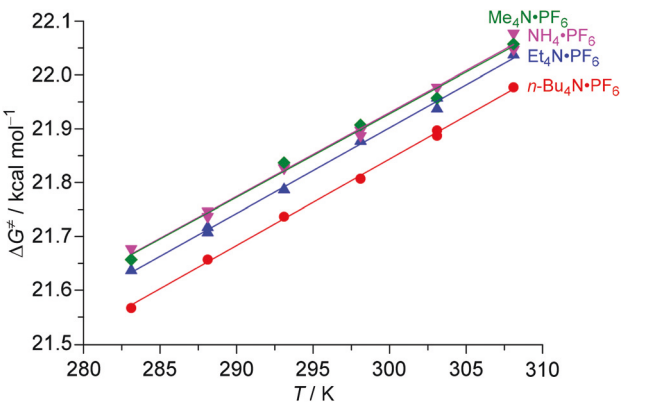

Fig. 8 The derived $\Delta G^{\ddagger}$ values as a function of temperature (T) for the switching of $\mathbf{1}^{5+/1\bullet}$ to $\mathbf{S1}^{5+/1\bullet}$ in the presence of different salts. Red, blue, purple and green lines correspond to n-Bu$_4$N·PF$_6$, Et$_4$N·PF$_6$, Me$_4$N·PF$_6$ and NH$_4$·PF$_6$, respectively. The slope and intercept of the linear regression give the values $-\Delta S^{\ddagger}$ and $\Delta H^{\ddagger}$, respectively, from the equation $\Delta G^{\ddagger} = \Delta H^{\ddagger} - T \times \Delta S^{\ddagger}$. (The derived $\Delta G^{\ddagger}$ values can be found in Table S1† for n-Bu$_4$N·PF$_6$, Table S3† for Et$_4$N·PF$_6$, Table S4† for Me$_4$N·PF$_6$ and Table S5† for NH$_4$·PF$_6$).

Table 3 Kinetic parameters[a] for the switching of CBPQT^{4+} from the TTF$^{\bullet+}$ unit in $\mathbf{1}^{5+/1\bullet}$ to the OP unit in $\mathbf{S1}^{5+/1\bullet}$ (MeCN, with no or 0.1 M salt) measured by UV-Vis-NIR absorption spectroscopy using the absorption band at 1040 nm as probe

Salt	k [$\times 10^{-4}$ s^{-1}] T = 298.0 K	n	R^2	$\Delta G^{\ddagger}$ [kcal mol^{-1}] T = 298.0 K	$\Delta H^{\ddagger}$ [kcal mol^{-1}]	$\Delta S^{\ddagger}$ [cal mol^{-1} K^{-1}]
—	3.65 ± 0.10	8	0.996	22.14 ± 0.03	17.09 ± 0.42	−16.95 ± 1.45
n-Bu$_4$N·PF$_6$	6.55 ± 0.18	8	0.999	21.82 ± 0.03	17.02 ± 0.36	−16.08 ± 1.24
n-Bu$_4$N·ClO$_4$	12.9 ± 0.84	7	0.997	21.39 ± 0.03	14.10 ± 0.90	−24.46 ± 3.12

[a] The errors were calculated[53] using $\Delta T = 0.3$ K and n is the number of data points used to calculate $\Delta H^{\ddagger}$ and $\Delta S^{\ddagger}$.

Table 4 Kinetic parameters[a] for the switching of $CBPQT^{4+}$ from the $TTF^{\bullet+}$ unit to the OP unit in $\mathbf{1}^{5+/1\bullet}$ (MeCN, with no or 0.1 M salt) measured by UV-Vis-NIR absorption spectroscopy using the absorption band at 1040 nm as probe

Salt	k [$\times 10^{-4}$ s^{-1}] T = 298.0 K	n	R^2	$\Delta G^{\ddagger}$ [kcal mol^{-1}] T = 298.0 K	$\Delta H^{\ddagger}$ [kcal mol^{-1}]	$\Delta S^{\ddagger}$ [cal mol^{-1} K^{-1}]
—	3.65 ± 0.10	8	0.996	22.14 ± 0.03	17.09 ± 0.42	−16.96 ± 1.45
$NH_4{\cdot}PF_6$	5.46 ± 0.22	5	0.989	21.90 ± 0.03	17.31 ± 0.51	−15.42 ± 1.72
$Me_4N{\cdot}PF_6$	5.56 ± 0.12	9	0.994	21.90 ± 0.03	17.26 ± 0.45	−15.58 ± 1.54
$Et_4N{\cdot}PF_6$	5.83 ± 0.11	8	0.998	21.87 ± 0.02	17.14 ± 0.22	−15.89 ± 0.77
n-$Bu_4N{\cdot}PF_6$	6.55 ± 0.18	8	0.999	21.82 ± 0.03	17.02 ± 0.36	−16.08 ± 1.24

[a] The errors were calculated[53] using ΔT = 0.3 K and n is the number of data points used to calculate $\Delta H^{\ddagger}$ and $\Delta S^{\ddagger}$.

effect. In this case, the change in enthalpy ($\Delta H^{\ddagger}$) and entropy ($\Delta S^{\ddagger}$) is much larger, meaning that an alternative switching mechanism cannot be ruled out. This could, for example, relate to the significant reduction in the binding affinity of TTF derivatives for $CBPQT^{4+}$ in the presence of excess n-$Bu_4N{\cdot}ClO_4$ compared with excess n-$Bu_4N{\cdot}PF_6$ or salt free conditions.[45]

We attempted to extend the study to additional anions, including ones larger than PF_6^-. However, we have yet to find another salt that is compatible with our methodology. The first oxidation potentials of n-$Bu_4N{\cdot}BPh_4$ and n-$Bu_4N{\cdot}BF_4$ are both lower than the first oxidation potential of $\mathbf{1}{\cdot}4PF_6{\cdot}$TTF and therefore these salts are unsuitable. Attempts to conduct experiments in the presence of n-$Bu_4N{\cdot}SbF_6$ resulted in precipitate formation, and acceptable UV-Vis-NIR spectra could not be obtained. We therefore chose instead to extend the study by investigating whether varying the nature of the added cation would affect the kinetics of $\mathbf{1}{\cdot}4PF_6$.

A series of PF_6^- salts with cations of decreasing size (*i.e.* tetraethylammonium (Et_4N^+), tetramethylammonium (Me_4N^+) and NH_4^+ (Tables S3–S5† and Fig. S5–S7†) was investigated and compared with n-$Bu_4N{\cdot}PF_6$ using the method described above. Fig. 8 shows the barriers ($\Delta G^{\ddagger}$) plotted as a function of temperature (T) from which the enthalpic ($\Delta H^{\ddagger}$) and entropic ($\Delta S^{\ddagger}$) contributions to the kinetic barrier were obtained; these values are shown in Table 4.

In agreement with our observations above, addition of excess PF_6^- salt resulted in a larger rate constant (k) for the switching of $CBPQT^{4+}$ compared to the absence of added salt. With the exception of n-$Bu_4N{\cdot}PF_6$, for which it is slightly larger, the calculated rate constants of all salts in the series lie within error of one another, although we note that the centre of the range does increase slightly as the cation size increases. This may warrant further investigation, but there is currently insufficient evidence to claim any significant relationship between the switching rate and cation size. Nevertheless, any possible difference in k associated with changing the cation is considerably smaller than that observed when comparing either no salt to any of the tested salts, or changing from PF_6^- to ClO_4^-. The kinetic barrier ($\Delta G^{\ddagger}$) shows no significant variation along the series of cations, nor do the enthalpic ($\Delta H^{\ddagger}$) or entropic ($\Delta S^{\ddagger}$) contributions to the barrier. We conclude that it is the nature of the anion that makes the most significant contribution to the kinetics of the switching process. We propose that this outcome relates to changes in the ion-pair equilibrium (*e.g.* $CBPQT^{4+} + 4X^- \rightleftarrows CBPQT{\cdot}4X$, where X^- is an anion), which alter the association of the anions with the tetracationic $CBPQT^{4+}$ macrocycle. This in turn will affect the binding affinity of $CBPQT^{4+}$ for the different stations and the relative stability of different translational isomers (and transition states), therefore changing the size of the kinetic barrier and the switching rate. Fig. 9 shows the absorption (A) at 1040 nm plotted against time (t) for all of the oxidation studies recorded at 298 K, *i.e.* with and without the different salts added. It is evident that the time it takes to fully oxidise $\mathbf{1}^{4+}$ to $\mathbf{1}^{5+/1\bullet}$ is also much shorter in the presence of the 0.1 M salts (<30 s for all salts tested *vs. ca.* 500 s without).†† This observation could be exploited when designing efficient electroactive systems for controlled motion, as it should allow for faster switching processes, where both the oxidation of a TTF unit and the switching movement of an encircling $CBPQT^{4+}$ can be accelerated by the addition of a salt.

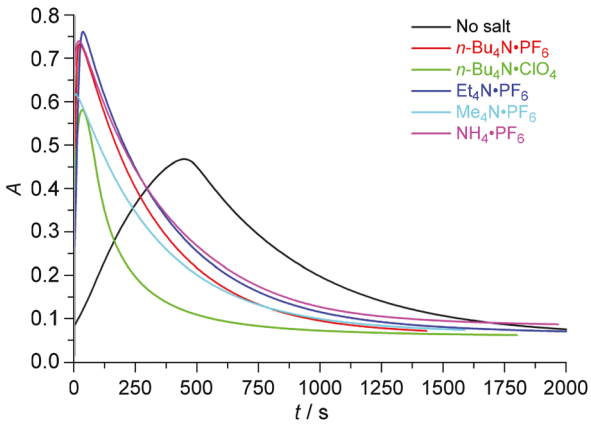

Fig. 9 The absorption (A) at 1040 nm after addition of 1.0 equiv. $Fe(ClO_4)_3$ to a solution of $\mathbf{1}{\cdot}4PF_6$ (0.1 mM) in MeCN (containing no or 0.1 M salt) at 298 K as a function of time (t).

Conclusion

Using UV-Vis-NIR absorption spectroscopy supported by cyclic voltammetry, we have investigated the mechanism and kinetics

†† Similar trends can be observed at all investigated temperatures.

of the switching process of the [2]rotaxane **1**·4PF_6 upon oxidation. In the ground state, **1**·4PF_6 exists almost exclusively as the 'unswitched' isomer with $CBPQT^{4+}$ around the central TTF station. Addition of a single equiv. of $Fe(ClO_4)_3$ enables the kinetics of the switching process to be determined for the oxidised [2]rotaxane $\mathbf{1}^{5+/1\bullet}$ where $CBPQT^{4+}$ moves between stations. It was observed that in the presence of all the 0.1 M salt solutions (*i.e.* a large excess), the rate constant associated with the switching process increased compared to the salt-free case. The rate of oxidation of the TTF unit also increased significantly. A series of PF_6^- salts with different ammonium cations (NH_4^+, Me_4N^+, Et_4N^+ and *n*-Bu_4N^+) increased the rate of switching by a factor of 1.5 to 1.8. The largest increase was observed for the largest cation, *n*-Bu_4N^+, but the obtained rate constants were very close to one another indicating that cation size has only a small effect, if any, on the kinetics. In contrast, when comparing *n*-$Bu_4N{\cdot}PF_6$ to *n*-$Bu_4N{\cdot}ClO_4$, a significant increase in the rate constant was observed when using the smaller ClO_4^- anion, to around 3.5 times that observed without added salt. We attribute these observations to changes to the ion-pair equilibrium in the presence of salts, which affect the binding affinity of $CBPQT^{4+}$ towards the stations in the dumbbell as well as helping to stabilise the transition state when $CBPQT^{4+}$ moves across the large SEt barrier. The addition of salts is a convenient method to increase switching rates in electroactive molecular shuttles based on $CBPQT^{4+}$, with the additional benefit of an increased oxidation rate. Faster switching has the potential to be a useful tool in the pursuit of efficient electroactive molecular machines exhibiting controlled motion, with applications such as molecular memory or drug delivery.

Experimental

General

All reagents used were standard grade and used as received. **1**·4PF_6,[32] **2**[32] and CBPQT·4PF_6 [38] were all prepared according to literature procedures. ^{1}H NMR spectra were recorded at 298 K on a Bruker AVANCE III spectrometer at 400 MHz. Chemical shifts are quoted on the δ scale. Samples for ^{1}H NMR spectroscopic studies were prepared using CD_3CN purchased from Sigma Aldrich. All spectra were referenced using the residual solvent peak. Ultraviolet–Visible-Near-InfraRed (UV-Vis-NIR) measurements were carried out on a Cary 5000 UV-Vis-NIR spectrophotometer. All experiments were carried out in air-equilibrated MeCN (HPLC grade) solutions. Temperature was controlled using an electronic thermostat. The estimated experimental errors are ±0.1% on the absorption (ΔA), ±0.1 s on the time (Δt) and ±0.3 K on the temperature (ΔT) unless otherwise stated.

Kinetic studies

A sample of [2]rotaxane **1**·4PF_6 dissolved in MeCN was transferred to a cuvette (3 mL) and heated or cooled to the desired temperature, followed by addition of 1.0 equiv. of $Fe(ClO_4)_3$ dissolved in MeCN. The addition of the oxidant results in the formation of a well-defined absorption band (1040 nm) assigned to the TTF radical cation ($TTF^{\bullet+}$) located inside the $CBPQT^{4+}$ ring, which then starts to diminish as a function of time as a consequence of the movement of $CBPQT^{4+}$ away from $TTF^{\bullet+}$. The UV-Vis-NIR spectrum of the solution was recorded before the addition of $Fe(ClO_4)_3$ and the absorption at 1040 nm was recorded every 10 s (or less) after the addition of the oxidant. The observed rate constant is four times the true rate constant, as a result of the disproportionation reaction and the possibility for $CBPQT^{4+}$ to move in two directions (see main text). When measurements were carried out in the presence of salts, a 0.1 M salt solution in MeCN was prepared and used in place of MeCN when making the solution of the [2]rotaxane **1**·4PF_6.

Cyclic voltammetry studies

Cyclic voltammetry (CV) experiments were carried out in nitrogen-purged MeCN or 1 : 2 DCE/MeCN (HPLC grade) solutions in a classical three-electrode, single-compartment cell at room temperature. The electrochemical cell was connected to a computerised potentiostat controlled by a personal computer. The working electrode was a glassy carbon electrode and its surface was polished immediately prior to use. A $Ag/AgNO_3$ electrode was used as the reference and a platinum wire was used as the counter electrode. The concentration of the examined compounds was 0.4 or 0.5 mM (see main text) with a tetrabutylammonium hexafluorophosphate (*n*-$Bu_4N{\cdot}PF_6$, 0.1 M) electrolyte. The measurements were carried out with a scan rate of 0.1 V s^{-1} at room temperature. Based on repeated measurements, absolute errors on potentials have been found to be less than ±0.01 V. A CV of ferrocene was recorded both prior to and after the measurements, showing an $E_{1/2}$ value equal to 0.084 V.

Conflicts of interest

There are no conflicts to declare.

Acknowledgements

This work was funded by Villum Foundation and the Danish Natural Science Research Council (FNU, Project 11-106744) in Denmark and AHF acknowledges support from the National Science Foundation (CHE 1709909).

Notes and references

1 Y.-C. You, M.-C. Tzeng, C.-C. Lai and S.-H. Chiu, *Org. Lett.*, 2012, **14**, 1046–1049.
2 J. W. Choi, A. H. Flood, D. W. Steuerman, S. Nygaard, A. B. Braunschweig, N. N. P. Moonen, B. W. Laursen, Y. Luo, E. DeIonno, A. J. Peters, J. O. Jeppesen, K. Xu,

J. F. Stoddart and J. R. Heath, *Chem. – Eur. J.*, 2006, **12**, 261–279.
3 M. Xue, Y. Yang, X. Chi, X. Yan and F. Huang, *Chem. Rev.*, 2015, **115**, 7398–7501.
4 D. A. Leigh, V. Marcos, T. Nalbantoglu, I. J. Vitorica-Yrezabal, F. T. Yasar and X. Zhu, *J. Am. Chem. Soc.*, 2017, **139**, 7104–7109.
5 Y. Wang, T. Cheng, J. Sun, Z. Liu, M. Frasconi, W. A. Goddard III and J. F. Stoddart, *J. Am. Chem. Soc.*, 2018, **140**, 13827–13834.
6 M. A. Jinks, A. de Juan, M. Denis, C. J. Fletcher, M. Galli, E. M. G. Jamieson, F. Modicom, Z. Zhang and S. M. Goldup, *Angew. Chem., Int. Ed.*, 2018, **57**, 14806–14810.
7 Z. Zhu, A. C. Fahrenbach, H. Li, J. C. Barnes, Z. Liu, S. M. Dyar, H. Zhang, J. Lei, R. Carmieli, A. A. Sarjeant, C. L. Stern, M. R. Wasielewski and J. F. Stoddart, *J. Am. Chem. Soc.*, 2012, **134**, 11709–11720.
8 J. M. Spruell, W. F. Paxton, J.-C. Olsen, D. Benitez, E. Tkatchouk, C. L. Stern, A. Trabolsi, D. C. Friedman, W. A. Goddard III and J. F. Stoddart, *J. Am. Chem. Soc.*, 2009, **131**, 11571–11580.
9 J. V. Hernández, E. R. Kay and D. A. Leigh, *Science*, 2004, **306**, 1532–1537.
10 S. Nygaard, S. W. Hansen, J. C. Huffman, F. Jensen, A. H. Flood and J. O. Jeppesen, *J. Am. Chem. Soc.*, 2007, **129**, 7354–7363.
11 A. Van Quaethem, P. Lussis, D. A. Leigh, A.-S. Duwez and C.-A. Fustin, *Chem. Sci.*, 2014, **5**, 1449–1452.
12 J. F. Stoddart, *Angew. Chem., Int. Ed.*, 2017, **56**, 11094–11125.
13 Z. Meng, J.-F. Xiang and C.-F. Chen, *Chem. Sci.*, 2014, **5**, 1520–1525.
14 S. F. M. van Dongen, S. Cantekin, J. A. A. W. Elemans, A. E. Rowan and R. J. M. Nolte, *Chem. Soc. Rev.*, 2014, **43**, 99–122.
15 M. R. Panman, C. N. van Dijk, A. Huerta-Viga, H. J. Sanders, B. H. Bakker, D. A. Leigh, A. M. Brouwer, W. J. Buma and S. Woutersen, *Nat. Commun.*, 2017, **8**, 2206.
16 S. Silvi, M. Venturi and A. Credi, *Chem. Commun.*, 2011, **47**, 2483–2489.
17 P. Ceroni, A. Credi and M. Venturi, *Chem. Soc. Rev.*, 2014, **43**, 4068–4083.
18 C. Gao, Z.-L. Luan, Q. Zhang, S. Yang, S.-J. Rao, D.-H. Qu and H. Tian, *Org. Lett.*, 2017, **19**, 1618–1621.
19 C. M. Keaveney and D. A. Leigh, *Angew. Chem., Int. Ed.*, 2004, **43**, 1222–1224.
20 A. Caballero, L. Swan, F. Zapata and P. D. Beer, *Angew. Chem., Int. Ed.*, 2014, **53**, 11854–11858.
21 T. A. Barendt, I. Rašović, M. A. Lebedeva, G. A. Farrow, A. Auty, D. Chekulaev, I. V. Sazanovich, J. A. Weinstein, K. Porfyrakis and P. D. Beer, *J. Am. Chem. Soc.*, 2018, **140**, 1924–1936.
22 T. Avellini, H. Li, A. Coskun, G. Barin, A. Trabolsi, A. N. Basuray, S. K. Dey, A. Credi, S. Silvi, J. F. Stoddart and M. Venturi, *Angew. Chem., Int. Ed.*, 2012, **51**, 1611–1615.
23 C. Pezzato, M. T. Nguyen, D. J. Kim, O. Anamimoghadam, L. Mosca and J. F. Stoddart, *Angew. Chem., Int. Ed.*, 2018, **57**, 9325–9329.
24 V. Serreli, L. Chin-Fa, E. R. Kay and D. A. Leigh, *Nature*, 2007, **445**, 523–527.
25 S. Di Motta, T. Avellini, S. Silvi, M. Venturi, X. Ma, H. Tian, A. Credi and F. Negri, *Chem. – Eur. J.*, 2013, **19**, 3131–3138.
26 S. Nygaard, B. W. Laursen, A. H. Flood, C. N. Hansen, J. O. Jeppesen and J. F. Stoddart, *Chem. Commun.*, 2006, **2**, 144–146.
27 A. Trabolsi, A. C. Fahrenbach, S. K. Dey, A. I. Share, D. C. Friedman, S. Basu, T. B. Gasa, N. M. Khashab, S. Saha, I. Aprahamian, H. A. Khatib, A. H. Flood and J. F. Stoddart, *Chem. Commun.*, 2010, **46**, 871–873.
28 K.-D. Zhang, X. Zhao, G.-T. Wang, Y. Liu, Y. Zhang, H.-J. Lu, X.-K. Jiang and Z.-T. Li, *Angew. Chem., Int. Ed.*, 2011, **50**, 9866–9870.
29 F. Durola and J.-P. Sauvage, *Angew. Chem., Int. Ed.*, 2007, **46**, 3537–3540.
30 H. Sugino, H. Kawai, T. Umehara, K. Fujiwara and T. Suzuki, *Chem. – Eur. J.*, 2012, **18**, 13722–13732.
31 C. Cheng, P. R. McGonigal, W.-G. Liu, H. Li, N. A. Vermeulen, C. Ke, M. Frasconi, C. L. Stern, W. A. Goddard III and J. F. Stoddart, *J. Am. Chem. Soc.*, 2014, **136**, 14702–14705.
32 S. S. Andersen, A. I. Share, B. La Cour Poulsen, M. Kørner, T. Duedal, C. R. Benson, S. W. Hansen, J. O. Jeppesen and A. H. Flood, *J. Am. Chem. Soc.*, 2014, **136**, 6373–6384.
33 A. Jana, S. Bähring, M. Ishida, S. Goeb, D. Canevet, M. Sallé, J. O. Jeppesen and J. L. Sessler, *Chem. Soc. Rev.*, 2018, **47**, 5614–5645.
34 L. J. O'Driscoll, J. M. Hamill, I. Grace, B. W. Nielsen, E. Almutib, Y. Fu, W. Hong, C. J. Lambert and J. O. Jeppesen, *Chem. Sci.*, 2017, **8**, 6123–6130.
35 M. Mansø, M. Koole, M. Mulder, I. J. Olavarria-Contreras, C. L. Andersen, M. Jevric, S. L. Broman, A. Kadziola, O. Hammerich, H. S. J. van der Zant and M. B. Nielsen, *J. Org. Chem.*, 2016, **81**, 8406–8414.
36 A. Coskun, J. M. Spruell, G. Barin, W. R. Dichtel, A. H. Flood, Y. Y. Botros and J. F. Stoddart, *Chem. Soc. Rev.*, 2012, **41**, 4827–4859.
37 J. O. Jeppesen, J. Perkins, J. Becher and J. F. Stoddart, *Angew. Chem., Int. Ed.*, 2001, **40**, 1216–1221.
38 M. Asakawa, W. Dehaen, G. Lábbé, S. Menzer, J. Nouwen, F. M. Raymo, J. F. Stoddart and D. J. Williams, *J. Org. Chem.*, 1996, **61**, 9591–9595.
39 J. O. Jeppesen and J. Becher, *Eur. J. Org. Chem.*, 2003, 3245–3266.
40 J. O. Jeppesen, J. Becher and J. F. Stoddart, *Org. Lett.*, 2002, **4**, 557–560.
41 R. Kristensen, S. S. Andersen, G. Olsen and J. O. Jeppesen, *J. Org. Chem.*, 2017, **82**, 1371–1379.
42 K. B. Simonsen and J. Becher, *Synlett*, 1997, 1211–1220.
43 M. B. Nielsen, C. Lomholt and J. Becher, *Chem. Soc. Rev.*, 2000, **29**, 153–164.

44 J. L. Segura and N. Martín, *Angew. Chem., Int. Ed.*, 2001, **40**, 1372–1409.
45 S. S. Andersen, M. Jensen, A. Sørensen, E. Miyazaki, K. Takimiya, B. W. Laursen, A. H. Flood and J. O. Jeppesen, *Chem. Commun.*, 2012, **48**, 5157–5159.
46 B. W. Laursen, S. Nygaard, J. O. Jeppesen and J. F. Stoddart, *Org. Lett.*, 2004, **6**, 4167–4160.
47 A. H. Flood, A. J. Peters, S. A. Vignon, D. W. Steuerman, H.-R. Tseng, S. Kang, J. R. Heath and J. F. Stoddart, *Chem. – Eur. J.*, 2004, **10**, 6558–6564.
48 A. C. Fahrenbach, J. C. Barnes, H. Li, D. Benítez, A. N. Basuray, L. Fang, C.-H. Sue, G. Barin, S. K. Dey, W. A. Goddard III and J. F. Stoddart, *Proc. Natl. Acad. Sci. U. S. A.*, 2011, **108**, 20416–20421.
49 I. Poleschak, J.-M. Kern and J.-P. Sauvage, *Chem. Commun.*, 2004, 474–476.
50 P. T. Kissinger and W. R. Heineman, *J. Chem. Educ.*, 1983, **60**, 702.
51 P. Farràs, E. C. Escudero-Adán, C. Viñas and F. Teixidor, *Inorg. Chem.*, 2014, **53**, 8654–8661.
52 A. H. Flood, S. Nygaard, B. W. Laursen, J. O. Jeppesen and J. F. Stoddart, *Org. Lett.*, 2006, **8**, 2205–2208.
53 N. Koumura, E. M. Geertsema, M. B. v. Gelder, A. Meetsma and B. L. Feringa, *J. Am. Chem. Soc.*, 2002, **124**, 5037–5051.